Sensitive Seismic Sensors Based on Microwave Frequency Fiber Interferometers in Commercially Deployed Cables: Supplementary material

Adonis Bogris[1], Thomas Nikas[2], Christos Simos[3], Iraklis Simos[4], Konstantinos Lentas[5], Nikolaos S. Melis[5], Andreas Fichtner[6], Daniel Bowden[6], Krystyna Smolinski[6], Charis Mesaritakis[7], Ioannis Chochliouros[8]

1. Dept. of Informatics and Computer Engineering, University of West Attica, Aghiou Spiridonos, 12243, Egaleo, Greece
2. Dept. of Informatics and Telecommunications, National and Kapodistrian University of Athens, Athens, GR-15784, Greece
3. Electronics & Photonics Laboratory, Dept. of Physics, University of Thessaly, 35100 Lamia, Greece
4. Department of Electrical and Electronics Engineering, University of West Attica, Aghiou Spiridonos, 12243, Egaleo, Greece
5. National Observatory of Athens, Institute of Geodynamics, Greece
6. Department of Earth Sciences, ETH Zurich, Switzerland
7. Dept. Information and Communication Systems Engineering, Engineering School, University of the Aegean, Palama 2, 83200, Samos, Greece
8. Hellenic Telecommunications Organization S.A. (OTE), 1, Pelika & Spartis, Maroussi, Athens, Greece

This document provides supplementary information to "Sensitive Seismic Sensors Based on Microwave Frequency Fiber Interferometers in Commercially Deployed Cables", including details on the processing of raw phase data, seismic data of various selected recorded earthquakes and a first analysis of the phase noise of the link and the individual building blocks/stages of the system.

A. Processing of phase data

One of the most significant units at the reception state is the one undertaking system monitoring and real-time calibration and processing of the data in order to seamlessly maximize the phase signal. At the reception stage, the microcontroller continuously monitors the output signal and calculates its real-time deviation with respect to the reference voltage level that corresponds to approximately $\pi/2$ phase difference between the microwave generator and the received signal, which maximizes sensitivity. When the real-time error voltage overcomes a specific threshold, a suitable control byte is sent to the HMC642ALC5 microwave phase shifter and the resulting phase transition restores operation close to maximum sensitivity. The signal is then post-processed in order to unwrap phase. Fig. 1a shows a snapshot of a raw signal recorded at the receiver where phase corrections are apparent as abrupt vertical transitions. In addition, specific bytes are used as flags to the recorded signal to ensure errorless phase unwrapping. Fig. 1b presents the phase unwrapped signal after post-processing. The arrow depicts the phase variation induced by the earthquake of Crete as an example (October 12, 2021, 09:24:03 UTC, (ML=6.3)) which is visible on the raw data before any post-processing.

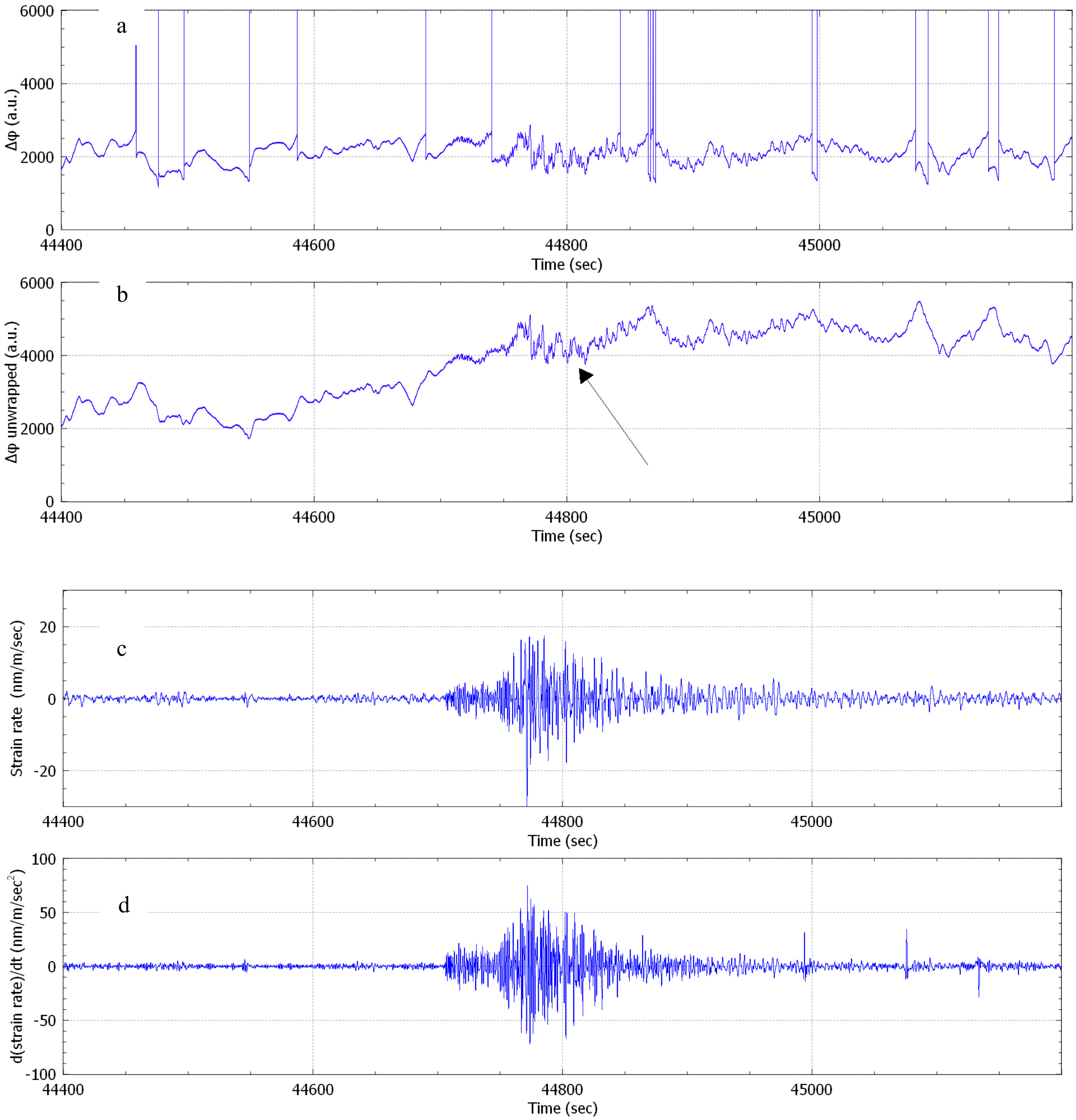

Fig. 1: Step by step processing of phase raw data – the phase shifter provides a continuous correction of the phase shift so as to maximize sensitivity (2000 mV correspond to π/2). a. Raw data, b. data after phase unwrapping, c. strain rate, d. 1st derivative of strain rate.

The output signal which is proportional to phase, is straightforwardly converted to strain by the equation:
$\varepsilon = \frac{dL}{L} = \frac{d\varphi}{\varphi} = \frac{c d\varphi}{2\pi n_g \xi f_{RF} L}$,
where $\xi \cong 0.78$ is the strain coefficient of the optical fiber due to the photoelastic effect. Further processing converts strain to strain rate ($\frac{d\varepsilon}{dt}$) or acceleration ($d^2\varepsilon/dt^2$) for comparison with seismometer or accelerometer recordings respectively (see Fig.1c, Fig.1d respectively).

It must be noted that such an active correction mechanism is more difficult to succeed when the phase of the link is interrogated using optical instead of microwave carriers, due to the rapid changes of phase as a result of environmental effects (optical phase variations exceeding decades of π per second are expected only due to temperature variations). Therefore, despite the fact that microwave frequencies are characterized by lower resolution compared to their optical counterparts, they are also more robust to link noise. This is one of the underlying reasons of MFFI efficacy in providing real-time measurements and consequently event detection in ms scale, despite its use in a noisy terrestrial link positioned in a densely populated area. We anticipate that its performance will be better in less noisy submarine links.

B. Recording of significant earthquake events

We selected more than ten significant earthquakes that took place during the system testing period (July 2021 to February 2022). In this document, we present the recordings from earthquakes with epicenters in Marousi, Ikaria, Kefalonia, Florina, Chalkidiki with epicenters depicted on the map in Figure 2, (left side) in the manuscript. The comparison between MFFI and ATHP data for the selected events are shown below. In all cases a satisfactory agreement is observed, especially noted for the horizontal components. It must be mentioned that MFFI records the seismic wave effect across a 25 km long link, whilst ATHP accelerometric station records the seismic wave at a specific point location. Our next goal is to install accelerometers along the specific link and study the correlation of the accumulated strain provided by the fiber with the superposition of the responses of the in-line accelerometers. This study will provide a better understanding of the strain distribution along the line and will guide us in transforming the MFFI technique to a distributed measurement technique.

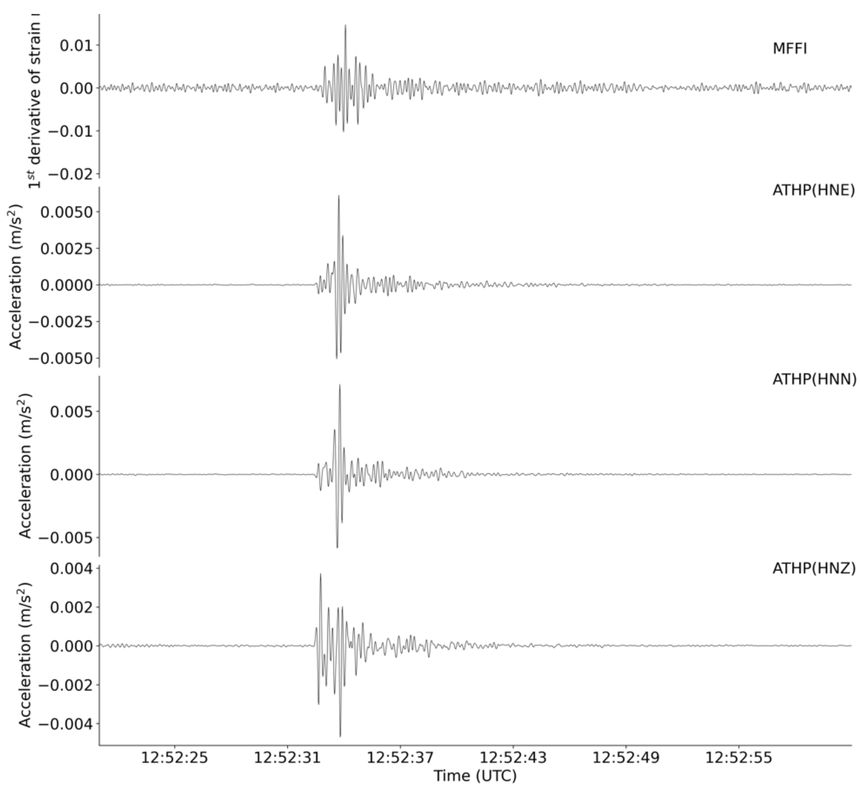

Fig. 2: Comparison of MFFI with ATHP records: Marousi, 25-10-2021, ML=2.8

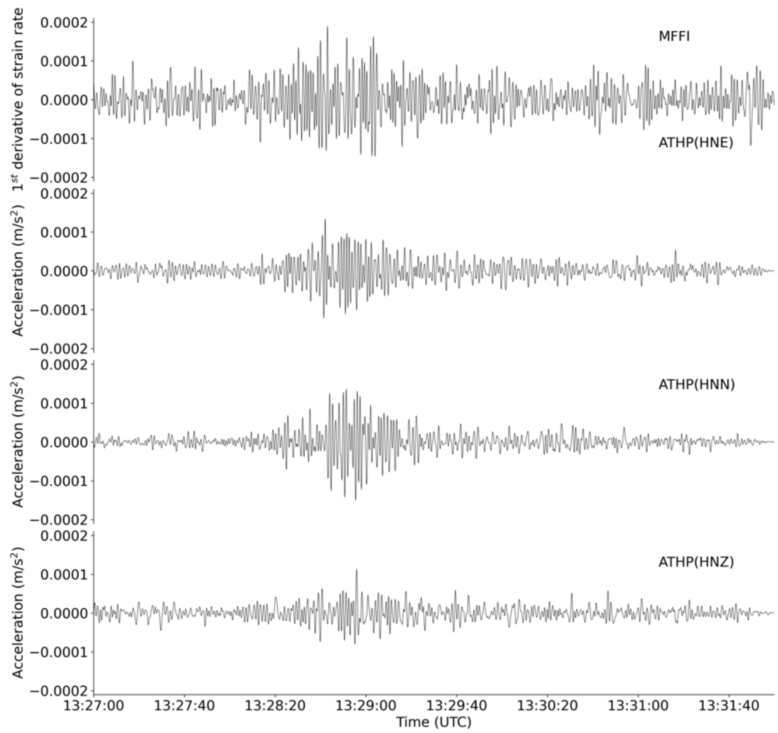

Fig. 3: Comparison of MFFI with ATHP records: Kefalonia, 19-11-2021, ML=4.8

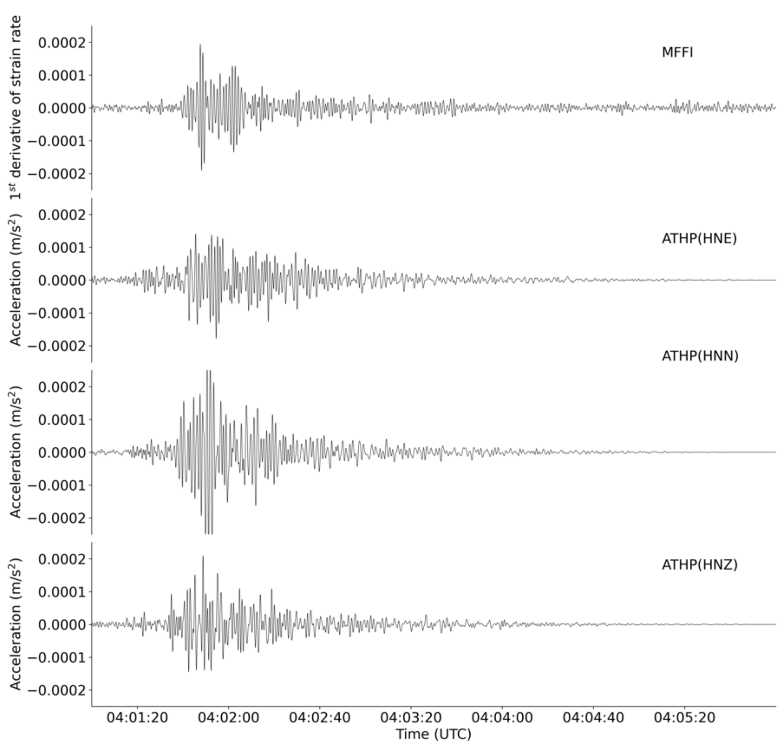

Fig. 4: Comparison of MFFI with ATHP records: Ikaria, 29-11-2021, ML=4.1

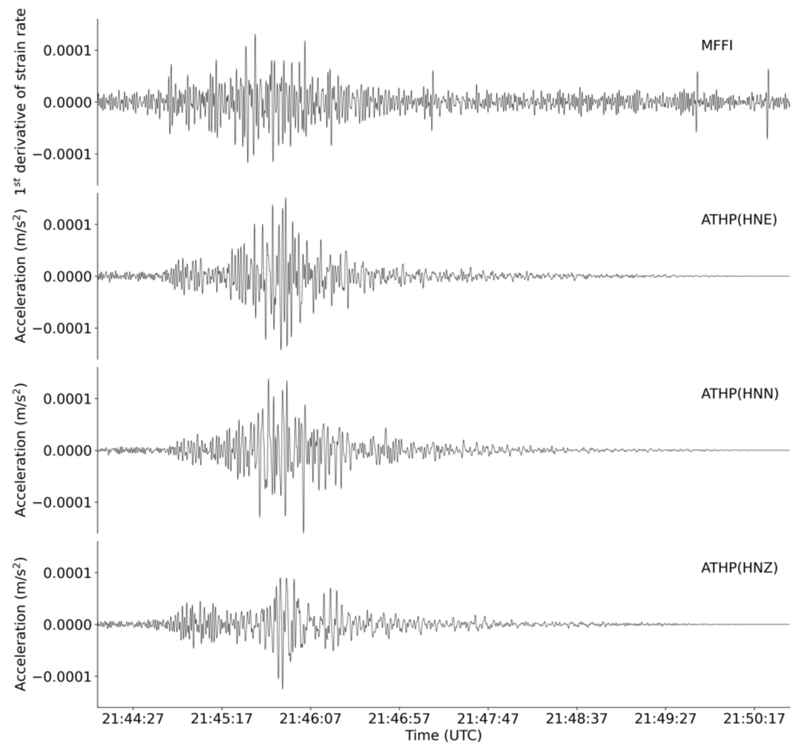

Fig. 5: Comparison of MFFI with ATHP records: Florina, 09-01-2022, ML=5.3

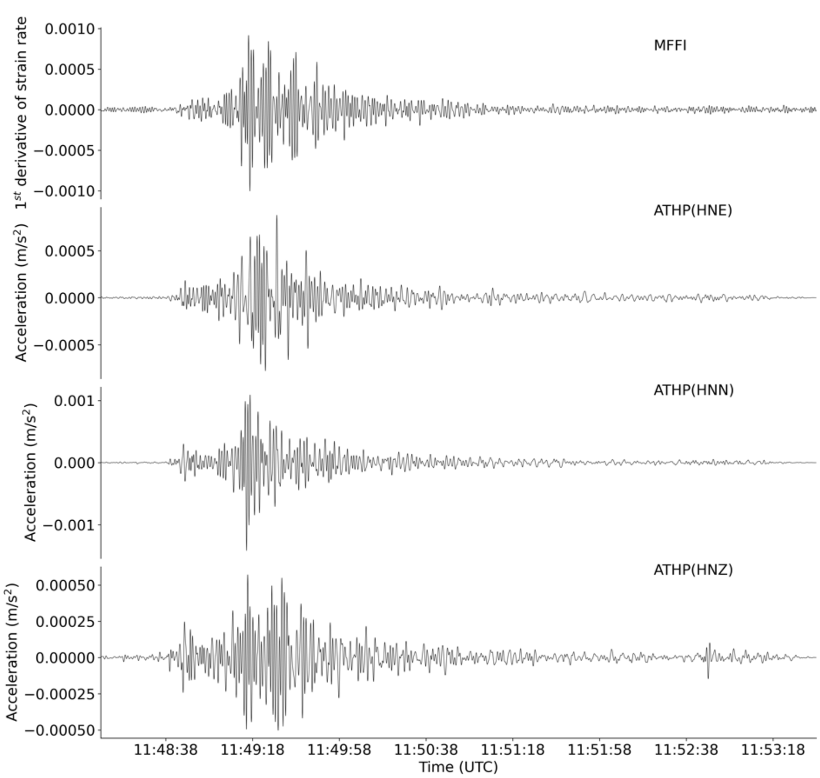

Fig. 6: Comparison of MFFI with ATHP records: Chalkidiki, 16-01-2022, ML=4.4

C. Phase noise of the terrestrial link and MFFI building blocks/stages

Here we present a study of the phase noise of the overall system including the fiber link, the optical and optoelectronic components (optical amplifiers, laser, and photodetector) and the noise of the electronic components (PLL, electrical amplifiers, mixers). We perform the analysis by measuring the one-sided spectral density of phase noise in dBc/Hz as depicted in Fig. 7. In all cases, the output signal is the one digitized by the 10-bit embedded analog to digital converter (ADC) of a low-cost micro-controller (Arduino Uno).

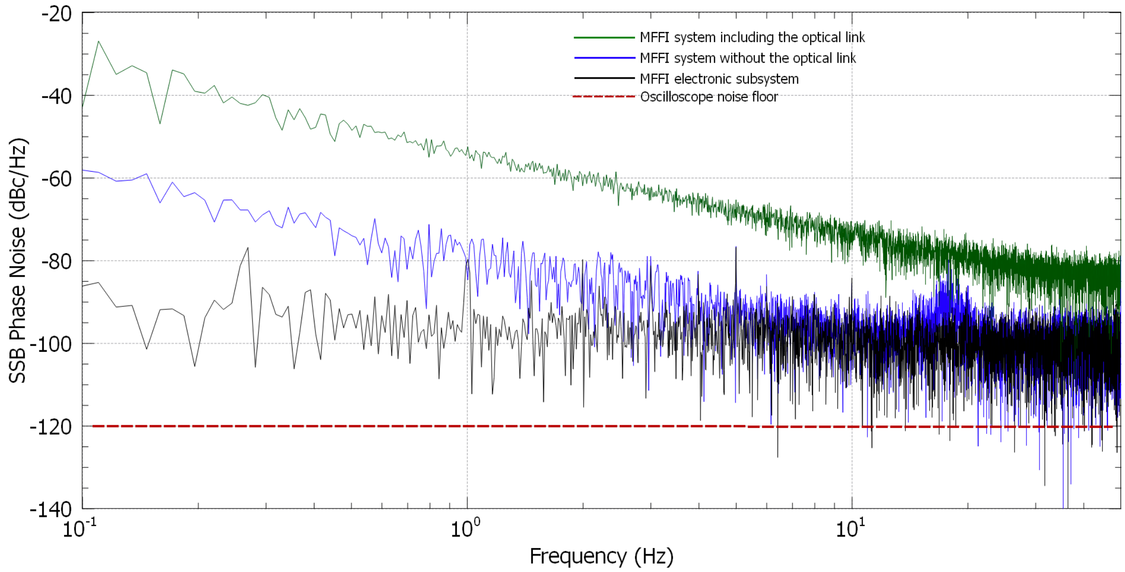

Fig. 7: SSB phase noise in dBc/Hz of MFFI output in various configurations (considered time = 100 sec) – no seismic wave is present in order to characterize the system in terms of the ordinary noise it is subjected to.

Green curve: The phase noise at the output of MFFI is measured when the entire link is included. The high-level spectral density at low frequencies is mostly attributed to link noise (temperature fluctuations, human activity)
Blue curve: The phase noise at the output of MFFI excluding the transmission link which has been replaced by optical attenuators in order to regulate the OSNR at the same level as in the green curve. It is obvious that phase noise has been reduced dramatically, although we observe strong components at low frequencies mostly due to the disturbance of optical components (patch-cords, EDFAs, etc) by mechanical/thermal vibrations inside OTE Academy building. Even at very low frequencies the spectral density of phase noise has been reduced by 20 dB.
Black curve: Here the phase noise is attributed only to the electronic part of the system; it corresponds to the noise floor of the measurement system. Hence the Arduino sampler quantization noise sets the lower limit of phase noise power spectral density approximately to -95 to -100 dBc/Hz.

When we measured the phase noise of the MFFI electronic subsystem with the use of an oscilloscope (Fig. 7 – dashed line) we obtained an improvement of 15-20 dB in the noise floor as depicted, which proves that a better sampling system could further improve MFFI's sensitivity, especially in less noisy environments. This is an improvement that will be applied in the next weeks, by substituting the Arduino 10-bit ADC of 50 Hz with a 14-bit 700 Hz ADC.